Investigation of Temporal Evolution of Hard X-Ray Spectrum from Neon-Seeded Plasma of ADITYA-U Tokamak*)

Shishir PUROHIT[1,2], Manoj K. GUPTA[1], Malay B. CHOWDHURI[1], Umesh NAGORA[1], Yashika TAUNK[1], Abhishek KUMAR[1], Kajal GARG[1], Surya K. PATHAK[1], Kumarpalsinh A. JADEJA[1], Rohit KUMAR[1], Kumudni TAHILIANI[1], Sameer KUMAR[1], Kaushal M. PATEL[1], Rakesh L. TANNA[1], Supriya A. NAIR[1], Joydeep GHOSH[1,2] and ADITYA-U Team

[1]*Institute for Plasma Research, Bhat, Gandhinagar 382428, Gujarat, India*
[2]*Homi Bhaba National Institute, Training School Complex, Anushakti Nagar, Mumbai 400094, India*

(Received 9 January 2023 / Accepted 18 July 2023)

The adverse effect associated with runaway electrons (RE) requires the temporal monitoring of the Hard X-ray (HX) spectrum produced by RE. This enables us to know the photon flux corresponding to a particular energy of HX in temporal space. A Lanthanum Bromide ($LaBr_3$)-based HX spectrometer system (80 keV ~ 5 MeV) is routinely operated on the ADITYA-U tokamak for monitoring the temporal evolution of the HX spectrum. The temporal evolutions of the HX energy having maximum count and the average RE temperature (RE average energy) have been analyzed for the plasmas injected with neon (Ne) impurity. It has been found that peak energy and average runaway energy reduces significantly after the Ne gas puff and this reduction happens when the electron density rises after the Ne gas puff. The RE temperature values were ~ 620 KeV and 230 KeV before and after the Ne injection, respectively. The spectral shape, in both counts and energy, shrunk drastically, suggesting the reduction of the HX emission after the Ne gas puffing.

Keywords: ADITYA-U, runaway electron, $LaBr_3$(Ce), neon seeding, runaway electron temperature

DOI: 10.1585/pfr.18.2402079

1. Introduction

Tokamak plasma devices under a long pulse operation are most likely subjected to large electromagnetic force, thermal and radiation loads on the plasma facing components (PFC), and first wall [1]. The risk is enhanced during the plasma disruption. A significant electric field present in the tokamak also has the potential to transform a non-zero population of the thermal electrons into a 'Runaway regime', runaway electrons (RE). RE experiences free acceleration with a small angle and long-range scattering which reduces the momentum transfer cross-sections [2]. This feature enables the RE to achieve very high energies and the current carried by RE can be substantially large. The RE current for ITER and the Demo devices are expected to be as high as a few tens of mega ampere [1]. These RE are capable enough to induce melting or deformation of the PFC due to their high energy. Hence, RE poses a substantial threat to the tokamak components as well as the thermal plasma. Therefore, a key interest is RE mitigation strategies which can increase momentum transfer from the RE to plasma and restrict the free acceleration of the plasma electrons. Several RE mitigation strategies have been suggested [3] out of which impurity seeding is one of the RE mitigation strategies, which not only performs RE mitigation along with increases plasma performance simultaneously [4]. However, to explore a suitable strategy for the mitigation, it is a prerequisite to understand the RE dynamic inside the plasma.

The Hard X-ray (HX) emissions made by the RE are the most efficient way to study the RE. Recently, HX spectroscopy has been picked up as one of the interesting candidates for the realization of RE energy [5, 6]. In a large tokamak, maximum efforts are devoted to understanding the disruption generated runaway electrons [4]. In addition to that, in the small and medium-sized tokamaks, HX spectroscopy has been carried out to investigate the primary and secondary generated RE during a plasma quiescent state.

HX spectroscopy studies have been conducted for impurity seeding experiments in ADITYA-U tokamak plasma to understand the RE behavior and dynamics. This investigation has been done using a recently installed Lanthanum Bromide ($LaBr_3$) based hard X-ray spectrometer capable of providing the temporal evolution of HX photon flux and energy simultaneously [5]. The work presented here addresses a novel approach to exploring the RE behavior as a function of the average RE energy and the spectral shape

author's e-mail: pshishir@ipr.res.in
malay@ipr.res.in

*) This article is based on the presentation at the 31st International Toki Conference on Plasma and Fusion Research (ITC31).

generated by the RE as a function of time. The results presented in this article assist in designing a RE mitigation strategy addressed to the reduction of the average RE energy. The experimental setup and a brief overview of the ADITYA-U tokamak are presented in Section 2. The results and discussions are presented in Section 3, where the temporal evolution of RE temperature (T_{eRE}) and its behavior with the amount of injected neon particles are presented. A summary is drawn in Section 4.

2. Experimental Set-Up

The ADITYA tokamak, which was a mid-sized circular poloidal limiter device having a large aspect ratio (R/a = 0.75 m/0.25 m = 3) and was operational for almost three decades, has been upgraded to ADITYA-U to perform experiments for understanding the RE dynamics, generation and mitigation relevant to big machines, like ITER and Demo devices. An additional toroidal belt limiter has been installed and special divertor coils have also been introduced for divertor shaped plasma operations. A wide variety of diagnostics are installed for better monitoring of the plasma with proper feedback control [7].

The temporal evolution of hard X-ray spectra is measured for ADITYA-U plasma by the ADITYA-U Hard X-ray Spectrometer (AUHXS) diagnostic, having an operational range of 80 keV ~ 5 MeV. It consists of a single-element $LaBr_3$(Ce) scintillator detector with the size of 1.5-inch × 1.5-inch and with an energy resolution of ~ 3% at 662 keV of Cs-137. The $LaBr_3$(Ce) scintillator detector of AUHXS is coupled with a 14-stage Hamamatsu photomultiplier tube, operated at 600 V. This section is connected with a data acquisition system (DAQ) i.e., a signal conditioning system and a multi-channel analyzer (MCA) integrated into a single unit, Canberra OSPREY. The OSPREY is capable of handling 250 kilo counts per second with remote operation via GENIE 2000 DAQ software. The GENIE 2000 is a plug and play software to operate OSPREY in MCA mode, where the counts and energy information of the spectra are available. However, with the assistance of a software development kit (SDK), the OSPREY is now operated in Time-List mode (TLIST), where counts, energy, and time information are available for every photon interacting with the detector. TLIST mode operation enables the realization of the temporal evolution of the 2 k channels HX spectrum [5].

AUHXS is viewing the plasma tangentially, with an outboard side poloidal limiter and an inboard side toroidal limiter in the field of view. The tangential viewing is adapted after carefully analyzing the benefits. In radial viewing of the plasma, which is perpendicular to the direction of the toroidal magnetic field (B_T), an accurate measurement of the high energy RE is almost impossible due to high anisotropy in X-ray bremsstrahlung. Tangential viewing is in a sense better than radial viewing, although the former also faces similar problems.

3. Results and Discussion

The analysis of HX spectra is conducted for the neon impurity seeding experiments in ADITYA-U [7]. A piezoelectric fast-closing valve is used to puff the neon gas. The neon reservoir pressure is kept almost constant for all the discharges and the height and width of the neon puff were varied to understand its effect on the temporal evolution of HX emission.

A typical ADITYA-U discharge (#34431) with neon seeding is presented in Fig. 1, having temporal evolution of plasma current (I_p) and loop voltage (V_L), soft X-ray (SX), and neutral hydrogen emission (H_α), electron density (n_e) and temperature (T_e), hard X-ray (HX) and average RE temperature (T_{eRE}). Two vertical lines represent the timing of two tiny pulses of neon gas puff having different applied voltages and pulse widths. The first neon puff is having a width of 1.1 ms (injecting ~ 10^{16} neon particles, which is ~ 0.15% of n_e in the discharge) and is injected into the plasma at ~ 102 ms. The electron density is 0.68×10^{19} m^{-3} and the electric field is 0.32 V/m just before the neon gas puff as shown in Fig. 1 (c). The electron density has risen to 0.82×10^{19} m^{-3} after the first neon puff and the electric field remains almost the same as indicated by nearly constant loop voltage before and after neon gas puff. The soft X-ray also rises and H_α reduces to a lower level. The HX signal in terms of MeV, in which every dot represents the energy of HX photon, reduces after the first neon puff as shown in Fig. 1 (d). For example, the number of counts corresponding to 2 MeV photon decrease after the first neon puff as compared to that before the puff as

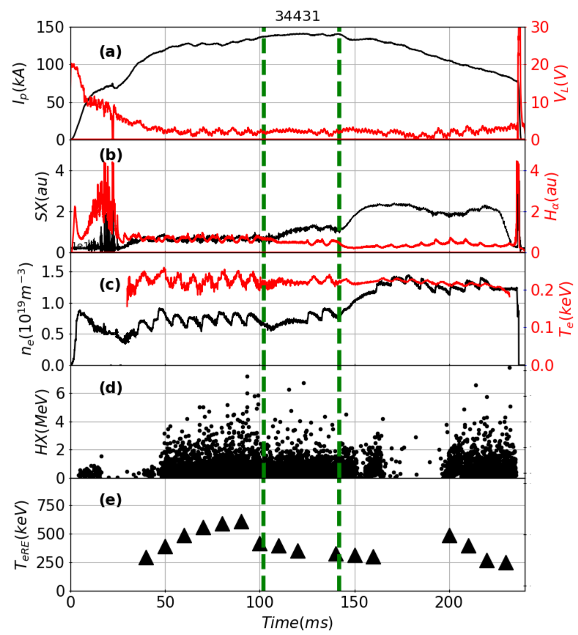

Fig. 1 The temporal evolution of (a) plasma current (I_p) and loop voltage (V_L), (b) soft X-ray (SX) and neutral hydrogen emission (H_α), (c) electron density (n_e) and temperature (T_e), (d) Hard X-ray (HX) and (e) average RE temperature (T_{eRE}) for an ADITYA-U discharge.

can be seen in Fig. 1 (e). The second puff is launched at ∼ 142 ms, the n_e is further raised from ∼ 0.83×10^{19} m^{-3} to ∼ 1.3×10^{19} m^{-3} at around 163 ms and the electric field is 0.32 V/m at this time. The electron temperature T_e does not change after the second neon puff. However soft X-ray signal has further elevated and the H_α signal reduced. The most vital observation from this experiment is that the HX signal has disappeared entirely for the times starting from 160 ms as the photon energy falls below the detection level of the detector (operational range 80 keV to 5 MeV). This directly indicates the substantial reduction of runaway electrons inside the plasma after the second neon puff. With the substantial rise in the density due to the neon seeding, the RE within the plasma has almost disappeared between 160 ms to 195 ms. It again reappears from 195 ms, when the plasma current drops significantly and loop voltage started increasing as the plasma becomes more resistive. The reason behind this appearance is not clear as of now. However, it might be related to the movement of the plasma column as the I_p has started dropping and the applied vertical field is pre-programmed, which leads to larger interaction between plasma facing components (PFC) and runaway electron. The behavior of HX is further investigated through the detailed analysis of HX spectra generated by the AUHXS. The two parameters, HX photon energy having maximum count, E_{peak}, and the average RE temperature, T_{eRE} have been obtained from the HX spectrum.

The HX spectrum is generated from the data of every HX photon energy (shown in Fig. 1 (d)) by integrating over 10 ms. The integration can be made over a shorter time window too, however, to increase the signal-to-noise ratio, a 10 ms second-time window is considered for this study. A typical set of HX spectra are plotted in Fig. 2 for discharge #34431. The spectra are taken at two discharge times at 98 and 122 ms, which are before and after the first neon puff, respectively. To get T_{eRE}, the spectrum is fitted with a line and the slope of the line gives the average runaway electron energy, referred to here as T_{eRE}. In the case of the spectrum at 98 ms, the spectral fitting is performed from 200 keV to ∼ 410 keV, which is considered to be the first slope after the peak in the spectrum. The spectral fitting for the spectra at 122 ms is done from 170 keV to 500 keV. The error in the estimation of the RE temperature is mainly due to the line fitting and is characterized by the R^2 values. The fitting error, R^2 values, for this study, remains between 0.92 - 0.95. Another parameter is E_{peak} which is the photon energy having maximum counts in the spectrum. E_{peak} lower value qualitatively indicates the improvement of the thermal content within the plasma. The E_{peak} for two spectra is marked by the vertical dashed line in Fig. 2. It is clear that as the discharge progresses, the energy value of the E_{peak} changes and moves towards the lower energy.

The temporal evolution of T_{eRE} is shown in Fig. 1 (e). Its value gradually increases as the discharge progresses

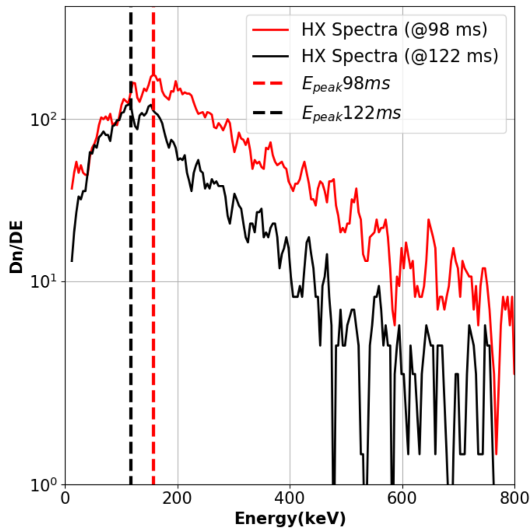

Fig. 2 The HX spectra for discharge #34431 at 98 ms and 122 ms. The vertical lines represent the E_{peak} for the two times.

and becomes the largest having a value of 750 keV just before the first neon puff. It reduces very much after the neon puff and its value comes down to ∼ 300 keV within a few ms of the first neon gas puffing. The T_{eRE} has a continuously decreasing trend and reduces to ∼ 250 keV at around 160 ms after the second puff. As The HX signal goes down the detection level, T_{eRE} cannot be estimated until 195 ms of the discharge. Later T_{eRE} could be estimated and its value become ∼ 500 keV and gradually reduces up to the times of discharge termination.

The HX spectrum acquired directly after the first neon gas puff has been analyzed from many similar discharges to understand the RE dynamics and behavior in the neon seeded plasmas. However, instead of analyzing the E_{peak} and T_{eRE} at a time after the neon gas puff, the difference between E_{peak} and T_{eRE} of two times, which are just before the first neon puff and at 20 ms after the first neon puff is analyzed.

Figure 3 presents a twin y-axis plot of the difference between pre and post-neon puff RE temperature i.e. $\Delta T_{eRE} = (T_{eRE})_{pre} - (T_{eRE})_{post}$, and $\Delta E_{peak} = (E_{peak})_{pre} - (E_{peak})_{post}$ on the respective y-axis. where the pre represents the T_{eRE}/E_{peak} just before the neon puff and the post represented the T_{eRE}/E_{peak} after the 20 ms of the first neon puff. The X-axis represent the number of injected neon particle during the first puff. It is seen that with the increase of the Ne particle, the ΔT_{eRE} increases as shown by red triangles. The number of Ne particles has increased almost twice (3.5 - 6.0), in the presented range, however, the ΔT_{eRE} has increased four times. This increase indicates the substantial reduction of runaway electron temperature after the first neon puff. The rise in the injected particle number also influences ΔE_{peak}, which represents the photon energy at the maximum count in the spectrum. The ΔE_{peak} shifts towards the lower energy side with the rising

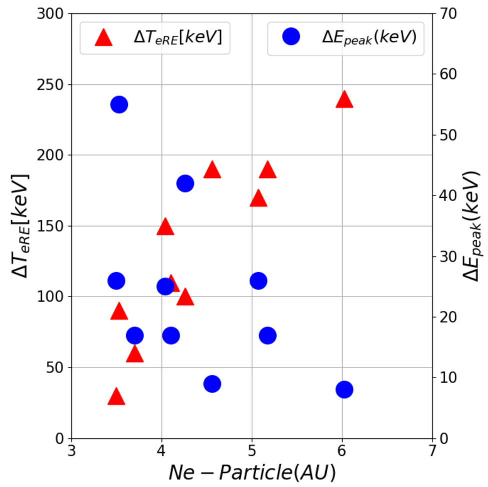

Fig. 3 ΔT_{eRE} and E_{peak} as a function of the neon particle.

particle injection. This indicates the improvement in the thermal character of the plasma.

The plasma electrons when overcomes the collisional drag, under an externally applied electric field in the toroidal direction ($E_{||}$), move to the runaway regime. This transformation of plasma electron to RE regime requires a sufficiently large electric field. The minimum required electric field for any electron to move to the RE regime is referred to as critical electric field E_C and is defined in equation 1 [3].

$$E_C = \frac{e^3 n_e \ln \Lambda}{4\pi\epsilon_0^2 m_e c^2}. \tag{1}$$

Where n_e is the electron density, $\ln \Lambda$ is the coulomb logarithm and all other notations have their usual meaning. Therefore, for non-zero RE population the $E_{||}/E_C > 1$, the toroidal electric field should be greater than the critical electric field. However, E_C does not have any dependency on the thermal electron temperature. Considering that, another type of electric field has been suggested, i.e., Dreicer electric field E_D, which is the minimum field required for the plasma thermal electron to migrate to the RE population as defined in equation 2 [3].

$$E_D = \frac{e^3 n_e \ln \Lambda}{4\pi\epsilon_0^2 k_b T_e}, \tag{2}$$

where T_e is electron temperature. The E_D shows a clear dependency on the electron temperature and poses an extra condition for RE generation [8,9]. The ΔT_{eRE} is shown in Fig. 4 as a function of the change in the Dreicer electric field, $\Delta E_D = ((E_D)_{pre} - (E_D)_{post})$. Here also, the Dreicer electric field of the pre and post neon puff times are estimated at the times, just before the first neon puff and at 20 ms after the first neon puff, respectively. As shown in Fig. 4, the ΔT_{eRE} is more when the required Dreicer electric field goes up substantially. This establishes the fact that fewer plasma electrons are now migrating to the RE regime. The density rises due to the neon puffing, increasing the required E_D. A higher electric field is now required to transform the confined plasma electron to the RE regime. The rise in the neon particle increases the electron density and the collisions within the plasma are expected to increase. Eventually, the required Dreicer field also increases. Not only, that, a considerable amount of plasma energy is also now consumed for the ionization and excitation of injected neon particles. All these processes work together to bring down the T_{eRE} and the E_{peak} moves at the lower energy side. This qualitatively suggests an increase in the overall thermal content of the plasma.

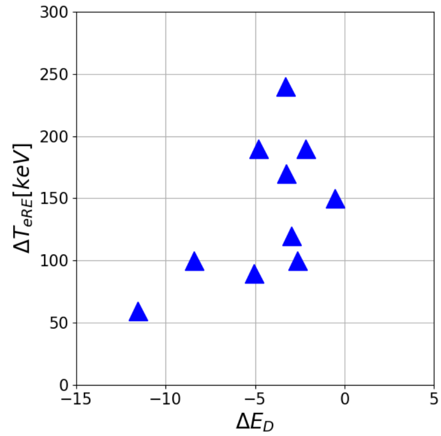

Fig. 4 ΔT_{eRE} as a function of the Dreicer Electric Field.

4. Summary

The neon seeding experiment was done in the ADITYA-U tokamak. The temporal evolution of the hard X-ray spectrum has been monitored using a $LaBr_3$ detector based hard X-ray spectrometer. The behavior of runaway electrons is investigated by obtaining two parameters, one is runaway electron energy, T_{eRE} and another is the E_{peak}, the energy at maximum counts. The analysis is carried out with the change in the injected neon particles and the required Dreicer electric field (E_D). It is observed that neon seeding substantially reduces the runaway electron temperature. The E_{peak} of hard X-ray spectra also moves towards the lower energy side with an increasing amount of neon puffing. Neon puffing increases the electron density which eventually gives rise to the required Dreicer electric field. As a consequence, the thermal electron content in the plasma seems to have improved.

[1] A. Hassanein and V. Sizyuk, Sci. Rep. **11**, 2069 (2021).
[2] B.N. Breizman *et al.*, Nucl. Fusion **59**, 83001 (2019).
[3] H. Knoepfel and D.A. Spong, Nucl. Fusion **19**, 785 (1979).
[4] M. Lehnen *et al.*, J. Nucl. Mater. **463**, 39 (2015).
[5] S. Purohit *et al.*, Rev. Sci. Instrum. **93**, 93512 (2022).
[6] V. Plyusnin *et al.*, Nucl. Fusion **46**, 277 (2006).
[7] R.L. Tanna *et al.*, Nucl. Fusion **62**, 42017 (2022).
[8] A. Shevelev *et al.*, Nucl. Fusion **61**, 116024 (2021).
[9] J.R. Martin-Solis *et al.*, Phys. Rev. Lett. **105**, 185002 (2010).